

# Impact of the valence band structure of $\text{Cu}_2\text{O}$ on excitonic spectra

Frank Schweiner, Jörg Main, Matthias Feldmaier, and Günter Wunner  
*Institut für Theoretische Physik 1, Universität Stuttgart, 70550 Stuttgart, Germany*

Christoph Uihlein  
*Experimentelle Physik 2, Technische Universität Dortmund, 44221 Dortmund, Germany*  
 (Dated: March 7, 2022)

We present a method to calculate the excitonic spectra of all direct semiconductors with a complex valence band structure. The Schrödinger equation is solved using a complete basis set with Coulomb Sturmian functions. This method also allows for the computation of oscillator strengths. Here we apply this method to investigate the impact of the valence band structure of cuprous oxide ( $\text{Cu}_2\text{O}$ ) on the yellow exciton spectrum. Results differ from those of J. Thewes *et al.* [Phys. Rev. Lett. **115**, 027402 (2015)]; the differences are discussed and explained. The difference between the second and third Luttinger parameter can be determined by comparisons with experiments, however, the evaluation of all three Luttinger parameters is not uniquely possible. Our results are consistent with band structure calculations. Considering also a finite momentum  $\hbar K$  of the center of mass, we show that the large  $K$ -dependent line splitting observed for the  $1S$  exciton state by G. Dasbach *et al.* [Phys. Rev. Lett. **91**, 107401 (2003)] is not related to an exchange interaction but rather to the complex valence band structure of  $\text{Cu}_2\text{O}$ .

PACS numbers: 71.35.-y, 78.20.-e, 02.20.-a, 71.20.Nr

## I. INTRODUCTION

Excitons are the quanta of the fundamental optical excitations in both insulators and semiconductors in the visible and ultraviolet spectrum of light. Being composed of an electron and a positively charged hole, Wannier excitons can be treated within the so-called simple band model as an analog of the hydrogen atom [1–4].

This simple band model assumes that both the valence band and the conduction band are parabolic, isotropic and nondegenerate. However, in all crystals with zincblende and diamond structure the valence band is degenerate at the center of the first Brillouin zone [5, 6]. Consequently, an interpretation of experimental spectra in terms of the hydrogen-like description of excitons is often not possible [7].

This is also true for cuprous oxide ( $\text{Cu}_2\text{O}$ ), which is one of the most interesting semiconductors relating to excitons due to the large excitonic binding energy of  $R_{\text{exc}} \approx 86$  meV [8, 9]. Only after Altarelli, Baldeschi and Lipari had developed the theory of excitons in semiconductors with degenerate valence bands in the 1970s [5, 10–13], a controversy regarding the correct assignment of the exciton states for  $\text{Cu}_2\text{O}$  could be settled by Ch. Uihlein *et al.* in 1981 [14], i.e., almost 30 years after the experimental discovery of excitons in  $\text{Cu}_2\text{O}$  by Gross and Karryjew [15].

Very recently, new attention has been drawn to the field of excitons by an experimental observation of the so-called yellow exciton series in  $\text{Cu}_2\text{O}$  up to a large principal quantum number of  $n = 25$  [16]. Besides a variety of new experimental and theoretical investigations on this topic [9, 17–19], the complex valence band structure of  $\text{Cu}_2\text{O}$  has also moved into the focus once again [8, 20].

In this paper we present a method to solve the cubic

Hamiltonian of excitons, which accounts for the complex valence band structure of most semiconductors. We solve the corresponding Schrödinger equation in a complete basis including the Coulomb-Sturmian functions, which also allows the direct calculation of oscillator strengths from the excitonic wave function and is not limited to certain quantum numbers as in previous works [5, 20]. Using this method we will reinvestigate the calculations of Ref. [20] to discuss the values of the three Luttinger parameters of  $\text{Cu}_2\text{O}$ . Deviations from previous results are observed and discussed. However, our method is of general applicability for all direct semiconductors with a complex valence band structure, e.g., GaAs [13], CuBr [21], and other compounds [10]. Only the values of the material parameters used have to be replaced. The decisive advantage of our method is the fact that it can also be used for the theoretical investigation of exciton spectra in external magnetic and electric fields, where the effects of the complex valence band structure are much more evident [7] and where other methods with a restricted amount of quantum numbers [13, 20] may be too imprecise or too complex due to the strong mixing of different exciton states. An application will be presented in Ref. [22].

In this paper will also show that a finite momentum  $\hbar K$  of the center of mass leads to terms in the Hamiltonian, which were initially assigned to the exchange interaction [23, 24]. These terms are of the correct order of magnitude to describe the  $K$ -dependent experimentally observed line splitting of the  $1S$  exciton [23, 24].

The paper is organized as follows: In Sec. II we present the theory of excitons for the case of degenerate valence bands. At first, we describe in Sec. II A the valence band structure and the yellow exciton series of  $\text{Cu}_2\text{O}$ . In this section we already discuss the impact of the band struc-

ture on the exciton series qualitatively. Having discussed the Hamiltonian of the exciton in Sec. II B, we introduce our complete basis in Sec. II C and describe how to calculate oscillator strengths in Sec. II D. We investigate the excitonic spectra in Sec. III A and discuss the values of the three Luttinger parameters. The treatment of the motion of the center of mass is presented in Sec. III B. Finally, we give a short summary and outlook in Sec. IV.

## II. THEORY

### A. Valence band structure and the yellow exciton series in $\text{Cu}_2\text{O}$

Concerning its hydrogen-like spectrum up to a principal quantum number of  $n = 25$  [16], the yellow exciton in  $\text{Cu}_2\text{O}$  seems to be a perfect example of a Wannier exciton. However, a more precise investigation of this spectrum shows clear deviations from the simple model with spherical effective masses [14, 20]. These deviations can be explained in terms of the complex valence band structure of  $\text{Cu}_2\text{O}$ .

Without spin-orbit coupling the valence band in  $\text{Cu}_2\text{O}$  has the symmetry  $\Gamma_5^+$  and is threefold degenerate at the  $\Gamma$ -point or the center of the Brillouin zone. This degeneracy can be accounted for by a quasi-spin  $I = 1$ , which is a convenient abstraction to denote the three orbital Bloch functions  $xy$ ,  $yz$ , and  $zx$ , which transform according to  $\Gamma_5^+$ . Since  $\text{Cu}_2\text{O}$  has cubic symmetry, the symmetry of the bands can be assigned by the irreducible representations  $\Gamma_i^\pm$  of the cubic group  $O_h$ , where the superscript  $\pm$  denotes the parity. Considering the spin-orbit coupling between the quasi-spin  $I$  and the spin  $S_h$  of a hole in the valence band, this sixfold degenerate band (now including the hole spin) splits into a lower lying fourfold-degenerate band ( $\Gamma_8^+$ ) and a higher lying twofold-degenerate band ( $\Gamma_7^+$ ) by an amount of  $\Delta$ , which is the spin-orbit coupling constant (see Fig. 1). The presence of the nonspherical symmetry of the solid as well as interband interactions cause these bands to be nonparabolic but deformed.

Neglecting these effects at first, one arrives at the simple-band model and can distinguish between four exciton series depending on the valence band and the conduction band involved (see Fig. 1). Within this model the wave function of an exciton consists of the so-called envelope function, which describes the relative movement of the electron and the hole, and the Bloch functions of the bands involved [3].

Due to the spins of electron and hole, e.g., the yellow exciton series is fourfold degenerate. The presence of an exchange interaction between the spins of the electron and the hole lifts this degeneracy and leads to ortho and para excitons [16, 25]. While the threefold degenerate ortho excitons can be observed in absorption spectra, the nondegenerate para excitons are spin-flip-forbidden [25].

Going now beyond the simple-band model, the anisotropic dispersion of the valence band has a signif-

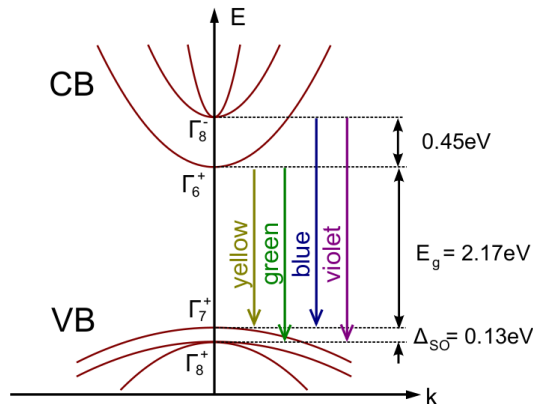


FIG. 1. (Color online) Band structure of  $\text{Cu}_2\text{O}$  [16]. Due to the spin-orbit coupling (2) the valence band splits into a lower lying fourfold-degenerate band ( $\Gamma_8^+$ ) and a higher lying twofold-degenerate band ( $\Gamma_7^+$ ). The lowest lying conduction band has  $\Gamma_6^+$  symmetry. Depending on the bands involved, one distinguishes between the yellow, green, blue, and violet exciton series.

icant influence on the excitons of the yellow series. The anisotropic dispersion leads to a coupling between the relative motion of the electron and the hole and the orbital Bloch functions  $xy$ ,  $yz$ , and  $zx$  [26] of the original  $\Gamma_5^+$ -band. This will be described mathematically by the so-called  $H_d$ -term in Sec. II C.

As can be seen from Fig. 1, the yellow exciton series is connected with the  $\Gamma_7^+$ -valence band. Due to symmetry considerations, the amplitudes, which describe the magnitude of the contribution of the orbital Bloch functions  $xy$ ,  $yz$  and  $zx$  to this band, must have the same absolute value. Thus, the anisotropy of the  $\Gamma_5^+$ -Bloch functions is compensated in the  $\Gamma_7^+$ -band. The same statement now also holds for all nondegenerate exciton states: for reasons of symmetry, the wave function of para excitons contains the orbital Bloch functions with amplitudes having the same absolute value. Thus, the dispersion of the para exciton can be described by an isotropic exciton mass.

As regards the threefold degenerate ortho exciton, the situation is different: each of the three exciton states can have a larger contribution of one of the orbital Bloch functions, respectively, without a violation of symmetry. The disparity in the orbital Bloch components of the ortho exciton is caused by an admixture of the  $\Gamma_8^+$ -valence band via the  $H_d$ -term. This disparity has then an impact on the relative motion of electron and hole. As a consequence, the envelope function of the ortho exciton has no further spherical or cubic symmetry but  $D_{4h}$ -symmetry. Since  $D_{4h}$  is a subgroup of  $O_h$ , it contains all symmetry operations, which leave a given  $\Gamma_5^+$ -component of the ortho exciton invariant. For instance, in the case of the  $xy$ -component the symmetry axis of the according subgroup  $D_{4h}$  is the  $z$ -axis of the crystal. So the reduction of the symmetry of the envelope function reflects

the anisotropic dispersion of the orbital Bloch functions. Due to the  $H_d$ -term the cubic symmetry  $O_h$  holds no further for the Bloch functions and the relative motion separately but only for the combined function.

The lower symmetry of the envelope function allows for a smaller mean distance between electron and hole in a specific direction, which leads to a gain of energy due to the Coulomb interaction. This effect may be compared to the Jahn-Teller effect, where a reduction of symmetry in connection with degeneracies leads to a gain of energy in the system.

As can be seen, there is a close connection between degeneracy and symmetry reduction of the envelope function. This fact explains one of the most striking features of excitonic spectra in  $\text{Cu}_2\text{O}$ : the visibility of  $D$  and  $F$  exciton states, i.e., exciton states with angular momentum  $L = 2$  and  $L = 3$  [14, 20]. The visibility arises due to the admixture of quadrupole or dipole-allowed  $S$ - and  $P$ -exciton states.

In the following sections II B and II C we will now introduce the problem of excitons in  $\text{Cu}_2\text{O}$  from a more mathematical point of view.

## B. Hamiltonian

Via  $\mathbf{k} \cdot \mathbf{p}$ -perturbation theory and symmetry considerations one can derive the Hamiltonian or the kinetic energy of an electron within the valence band structure described in Sec. II A [8, 25, 27]:

$$\begin{aligned} H_{\text{vb}}(\mathbf{k}) = & -H_{\text{so}} + (1/2m_0) \{ \mathbf{k}^2 [\hbar^2 A_1 + 2B_1 (\mathbf{I} \mathbf{S}_h)] \\ & + A_2 (k_1^2 (\mathbf{I}_1^2 - \mathbf{I}^2/3) + \text{c.p.}) \\ & + B_2 (2k_1^2 (\mathbf{I}_1 \mathbf{S}_{h1} - \mathbf{I} \mathbf{S}_h/3) + \text{c.p.}) \\ & + A_3 (2 \{k_1, k_2\} \{ \mathbf{I}_1, \mathbf{I}_2 \} + \text{c.p.}) \\ & + B_3 (2 \{k_1, k_2\} (\mathbf{I}_1 \mathbf{S}_{h2} + \mathbf{I}_2 \mathbf{S}_{h1}) + \text{c.p.}) \} \quad (1) \end{aligned}$$

with  $\{a, b\} = \frac{1}{2}(ab + ba)$ , the free electron mass  $m_0$ , and c.p. denoting cyclic permutation. The spin-orbit coupling reads [14, 20]

$$H_{\text{so}} = \frac{2}{3} \Delta \left( 1 + \frac{1}{\hbar^2} \mathbf{I} \mathbf{S}_h \right). \quad (2)$$

Note that we use, in contrast to Ref. [8], the energy shift of  $2\Delta/3$ , by which the energy of the  $\Gamma_7^+$ -band is set to zero at the  $\Gamma$ -point. Furthermore, we use the spin matrices of spin 1/2 for the hole spin instead of the Pauli matrices. The matrices of the quasi-spin  $I = 1$  are defined as in Ref. [27],

$$\mathbf{I}_k = \sum_{l,m} -i\hbar \varepsilon_{klm} (\hat{e}_l \otimes \hat{e}_m), \quad (3)$$

with the unit vectors  $\hat{e}_i$  and the Levi-Civita symbol  $\varepsilon_{klm}$ .

TABLE I. Material parameters used in the calculations. In Sec. III A we use two different sets of the parameters  $\Delta$ ,  $\gamma_1$ , and  $\mu'$ . For further information see text.

Band gap energy	$E_g = 2.17028 \text{ eV}$	[16]
Electron mass	$m_e = 0.99 m_0$	[34]
Dielectric constant	$\varepsilon = 7.5$	[35]
Exchange interaction	$J_0 = 12 \text{ meV}$	[8]
Spin-orbit coupling	$\Delta = 0.131 \text{ eV}$	[8]
Valence band parameters	$\gamma_1' = 2.77$	[8]
	$\mu' = 0.0586$	[8]
	$\eta_1 = -0.02$	[8]
	$\nu = 2.167$	[8]
	$\tau = 1.5$	[8]
Spin-orbit coupling	$\Delta = 0.1338 \text{ eV}$	[14,20]
Valence band parameters	$\gamma_1' = 2.78$	[14,20]
	$\mu' = 0.47$	[14,20]

Very recently, the parameters  $A_i$  and  $B_i$  in Eq. (1) have been obtained [8] by fitting the Hamiltonian to results of band structure calculations [30]:

$$A_1 = -1.76, \quad A_2 = 4.519, \quad A_3 = -2.201, \quad (4a)$$

$$B_1 = 0.02, \quad B_2 = -0.022, \quad B_3 = -0.202. \quad (4b)$$

In the case of an exciton one generally treats the missing electron in the valence band as a hole, i.e., a quasi-particle with an energy being opposite to the energy of the other electrons in the valence band. Using the definition of the three Luttinger parameters,

$$\gamma_1 = -A_1, \quad \gamma_2 = \frac{1}{6} A_2, \quad \gamma_3 = \frac{1}{6} A_3, \quad (5a)$$

and defining by analogy

$$\eta_1 = -B_1, \quad \eta_2 = \frac{1}{6} B_2, \quad \eta_3 = \frac{1}{6} B_3, \quad (5b)$$

the Hamiltonian of the hole reads [20, 25, 31, 32]

$$\begin{aligned} H_h(\mathbf{p}) = & H_{\text{so}} + (1/2\hbar^2 m_0) \{ \hbar^2 (\gamma_1 + 4\gamma_2) \mathbf{p}^2 \\ & + 2(\eta_1 + 2\eta_2) \mathbf{p}^2 (\mathbf{I} \mathbf{S}_h) \\ & - 6\gamma_2 (p_1^2 \mathbf{I}_1^2 + \text{c.p.}) - 12\eta_2 (p_1^2 \mathbf{I}_1 \mathbf{S}_{h1} + \text{c.p.}) \\ & - 12\gamma_3 (\{p_1, p_2\} \{ \mathbf{I}_1, \mathbf{I}_2 \} + \text{c.p.}) \\ & - 12\eta_3 (\{p_1, p_2\} (\mathbf{I}_1 \mathbf{S}_{h2} + \mathbf{I}_2 \mathbf{S}_{h1}) + \text{c.p.}) \}. \quad (6) \end{aligned}$$

The parameters in Eq. (6) describe the dispersion of the hole in the vicinity of the  $\Gamma$ -point:  $\gamma_1$  and  $\eta_1$  determine the average effective mass of the hole while the other parameters describe the splitting of the bands in the vicinity of the  $\Gamma$ -point and the so-called band warping or the nonspherical symmetry of the bands [25].

The Hamiltonian of the exciton is given by [5, 14]

$$H = E_g + H_e(\mathbf{p}_e) + H_h(\mathbf{p}_h) + V + H_{\text{exch}} + H_C \quad (7)$$

with the energy  $E_g$  of the band gap and the kinetic energy of the electron,

$$H_e(\mathbf{p}_e) = \frac{\mathbf{p}_e^2}{2m_e}. \quad (8)$$

Here  $m_e$  denotes the effective mass of the electron. The Coulomb interaction, which is screened by the dielectric constant  $\varepsilon$ , reads

$$V(\mathbf{r}_e - \mathbf{r}_h) = -\frac{e^2}{4\pi\varepsilon_0\varepsilon} \frac{1}{|\mathbf{r}_e - \mathbf{r}_h|}. \quad (9)$$

The last two terms of Eq. (7) are given by [14, 33, 34]

$$H_{\text{exch}} = J_0 \left( \frac{1}{4} - \frac{1}{\hbar^2} \mathbf{S}_e \mathbf{S}_h \right) \delta(\mathbf{r}) \quad (10)$$

and [35]

$$H_C = \frac{a^2}{24\hbar^2} \left( \frac{c_e}{m_e} \mathbf{p}_e^4 + \frac{c_h}{m_h} \mathbf{p}_h^4 \right) - d \frac{e^2 a^2}{\varepsilon_0 \varepsilon^2} \delta(\mathbf{r}_e - \mathbf{r}_h) \quad (11)$$

and denote the exchange interaction as well as the central-cell corrections. The coefficients  $c_e = 1.35$ ,  $c_h = 1.35$ , and  $d = 0.18$  were calculated in Ref. [35] within the simple band model and with  $m_h = 0.69 m_0$  for the hole mass. Here  $a = 4.26 \times 10^{-10}$  m is the lattice constant.

In the case of the  $1S$  exciton, i.e., the ground state of the exciton, the wave function is highly localized in position space and comprises only a few unit cells of the solid, for which reason terms of the order four in the momentum have to be considered. Besides the  $\mathbf{p}^4$ -terms in Eq. (11), one could also imagine terms of the form  $p_1^4 + p_2^4 + p_3^4$ , which have cubic symmetry. The last term in Eq. (11) appears due to corrections in the dielectric constant since the continuum approach is not valid for the  $1S$  exciton.

For subsequent calculations it is appropriate to write the Hamiltonian (7) in terms of irreducible tensors [12, 36, 37], where we additionally set the position and the momentum of the center of mass to zero:

$$\begin{aligned} H = & E_g - \frac{e^2}{4\pi\varepsilon_0\varepsilon} \frac{1}{r} + \frac{2}{3} \Delta \left( 1 + \frac{1}{\hbar^2} I^{(1)} \cdot S_h^{(1)} \right) + H_{\text{exch}} + H_C \\ & + \frac{\gamma'_1}{2\hbar^2 m_0} \left[ \hbar^2 p^2 - \frac{\mu'}{3} P^{(2)} \cdot I^{(2)} + \frac{\delta'}{3} \left( \sum_{k=\pm 4} [P^{(2)} \times I^{(2)}]_k^{(4)} + \frac{\sqrt{70}}{5} [P^{(2)} \times I^{(2)}]_0^{(4)} \right) \right] \\ & + \frac{3\eta_1}{\hbar^2 m_0} \left[ \frac{1}{3} p^2 \left( I^{(1)} \cdot S_h^{(1)} \right) - \frac{\nu}{3} P^{(2)} \cdot D^{(2)} + \frac{\tau}{3} \left( \sum_{k=\pm 4} [P^{(2)} \times D^{(2)}]_k^{(4)} + \frac{\sqrt{70}}{5} [P^{(2)} \times D^{(2)}]_0^{(4)} \right) \right] \quad (12) \end{aligned}$$

The first-order and second-order tensor operators correspond, as in Ref. [37], to the vector operators  $\mathbf{r}$ ,  $\mathbf{I}$ ,  $\mathbf{S}_{e/h}$ , and to the second-rank Cartesian operators

$$I_{mn} = 3 \{I_m, I_n\} - \delta_{mn} I^2, \quad (13a)$$

$$P_{mn} = 3 \{p_m, p_n\} - \delta_{mn} p^2, \quad (13b)$$

respectively. We also use the abbreviation

$$D_k^{(2)} = \left[ I^{(1)} \times S_h^{(1)} \right]_k^{(2)}. \quad (14)$$

The coefficients  $\gamma'_1$ ,  $\mu'$ , and  $\delta'$  are given by [12, 14]

$$\gamma'_1 = \gamma_1 + \frac{m_0}{m_e}, \quad \mu' = \frac{6\gamma_3 + 4\gamma_2}{5\gamma'_1}, \quad \delta' = \frac{\gamma_3 - \gamma_2}{\gamma'_1} \quad (15a)$$

and we define by analogy

$$\nu = \frac{6\eta_3 + 4\eta_2}{5\eta_1}, \quad \tau = \frac{\eta_3 - \eta_2}{\eta_1}. \quad (15b)$$

Since  $\eta_i \ll \gamma_i$  holds in Eq. (6), we neglect the corresponding terms of the Hamiltonian (12) in the following and use them only for the calculations at the end of Sec. III A. The material parameters used in our calculations are listed in Table I.

The parameters taken from Ref. [14] have been obtained as fit parameters to excitonic spectra using the spherical model, i.e., the model in which the  $\delta'$ -dependent terms are neglected. Recent calculations on the band structure of  $\text{Cu}_2\text{O}$  [30] yielded different values for the corresponding material parameters [8] showing that the spherical model by which  $\mu' = 0.47$  had been obtained may be inappropriate since  $|\delta'| \gg |\mu'|$  holds. These parameters are listed in Table I, as well.

### C. Choice of the basis set

To find an appropriate basis set to solve the Schrödinger equation, we have to discuss the different

terms of the Hamiltonian (12) as in Ref. [14]. The Hamiltonian

$$H_{\text{sb}} = E_g - \frac{e^2}{4\pi\epsilon_0\epsilon} \frac{1}{r} + \frac{\gamma'_1}{2m_0} p^2 + H_C \quad (16)$$

is the hydrogen-like Hamiltonian of the simple-band model. Without the central-cell corrections, which here account for the deviations of the exciton ground state from the hydrogen-like series, the solutions of  $H_{\text{sb}}$  are given by

$$E_n = E_g - \frac{R_{\text{exc}}}{n^2} \quad (17)$$

with the principal quantum number  $n$  and the excitonic Rydberg energy  $R_{\text{exc}}$  [25]. The eigenfunctions are the well-known solutions of the Schrödinger equation of the hydrogen atom, where only the Bohr radius  $a_0$  is to be replaced by the excitonic radius  $a_{\text{exc}} = \epsilon\gamma'_1 a_0$  [25].

The spin-orbit interaction  $H_{\text{so}}$  couples the quasi-spin  $I = 1$  and the hole spin  $S_h = 1/2$  to the effective hole spin  $J = I + S_h$ , where  $J = 1/2$  corresponds to the  $\Gamma_7^+$  valence band and  $J = 3/2$  corresponds to the  $\Gamma_8^+$  valence bands. The value of  $J$  therefore distinguishes between the yellow ( $J = 1/2$ ) and the green ( $J = 3/2$ ) exciton series (Fig. 1). Within this approximation, these are two noninteracting hydrogen-like exciton series.

The remaining parts of  $H$  without the exchange interaction form the so-called  $H_d$  term:

$$H_d = \frac{\gamma'_1}{2\hbar^2 m_0} \left\{ -\frac{\mu'}{3} P^{(2)} \cdot I^{(2)} + \frac{\delta'}{3} \left( \sum_{k=\pm 4} \left[ P^{(2)} \times I^{(2)} \right]_k^{(4)} + \frac{\sqrt{70}}{5} \left[ P^{(2)} \times I^{(2)} \right]_0^{(4)} \right) \right\}. \quad (18)$$

This term mixes the two exciton series as discussed in Sec. II A. In the spherical approximation ( $\delta' = 0$ ), in which the Hamiltonian has still spherical symmetry, the momentum  $F = L + J$  and its  $z$ -component  $M_F$  are good quantum numbers, while  $L$  and  $J$  do not commute with  $H_d$ . This leads to a fine-structure splitting of the eigenstates of the Hamiltonian, which is discussed, e.g., in Refs. [5, 12, 14] for several semiconductors. The angular momentum part of an appropriate basis set reads

$$|L; (I, S_h), J; F, M_F\rangle |S_e, M_{S_e}\rangle, \quad (19)$$

where the  $z$ -component  $M_{S_e}$  of the electron spin  $S_e = 1/2$  is also a good quantum number.

The other parts of  $H_d$  with the coefficient  $\delta'$  have cubic symmetry. For this reason neither  $F$  nor  $M_F$  are good quantum numbers anymore [11]. The eigenstates of the Hamiltonian transform according to the irreducible representation  $\Gamma_i^\pm$  of the cubic group  $O_h$  instead of those of the full rotation group.

In the case in which the value of an arbitrary (integral or half-integral valued) momentum  $A$  is less than or equal to four, it is possible to form linear combinations of the states  $|A, M_A\rangle$  that transform according to the irreducible representations of  $O_h$  [20, 26]. For example, the state  $(|3, 2\rangle - |3, -2\rangle)/\sqrt{2}$  transforms according to the irreducible representation  $\Gamma_2^-$  of  $O_h$ . These states are often denoted by  $|A, \Gamma_i\rangle$  [11]. However, this procedure is not uniquely possible for  $A > 4$  due to arising degeneracies [26]. Therefore, it is reasonable to describe the angular-momentum part by Eq. (19) even if  $\delta' \neq 0$  holds.

The effect of  $H_d$  on the eigenstates of the Hamiltonian decreases with increasing principal quantum number  $n$  since the wave functions extend over more unit cells and the cubic symmetry of the solid becomes less important [20]. An approach to treat the effects of  $H_d$

on exciton states with high values of  $n$  in a simple way can be found in Ref. [8].

The exchange interaction  $H_{\text{exch}}$  couples the spins of electron and hole and leads to a splitting of  $S$  excitons, i.e., excitons with  $L = 0$ , into ortho and para excitons [14]. The coupling of the spins leads to a total momentum  $F_t = F + S_e$  and we finally obtain

$$|L; (I, S_h), J; F, S_e; F_t, M_{F_t}\rangle \quad (20)$$

for the angular momentum part of an appropriate basis set.

In the literature the radial part of the basis is often not specified. A typical ansatz for the wavefunction of the exciton is

$$\Psi = \sum_{\beta} g_{\beta}(r) |L; (I, S_h), J; F, S_e; F_t, M_{F_t}\rangle, \quad (21)$$

where  $\beta$  denotes the quantum numbers  $L, J, F, F_t$ , and  $M_{F_t}$ . The radial functions  $g_{\beta}(r)$  are often determined using finite-element methods [14, 21] or variational methods [5, 11–13, 38]. Unfortunately, these methods lead to a huge number of coupled differential equations for the functions  $g_{\beta}(r)$ .

In contrast to earlier works, in this paper we use a complete basis for the radial functions. Since the eigenfunctions of the hydrogen atom do not represent a complete basis without the continuum states, we use the so-called Coulomb-Sturmian functions as described, e.g., in Ref. [39]. The radial functions of this basis read

$$U_{NL}(r) = N_{NL} (2\rho)^L e^{-\rho} L_N^{2L+1}(2\rho) \quad (22)$$

with  $\rho = r/\alpha$ , a normalization factor  $N_{NL}$ , the associated Laguerre polynomials  $L_n^m(x)$ , and an arbitrary scaling

parameter  $\alpha$ . Note that we here use the radial quantum number  $N$ , which is related to the principal quantum number  $n$  via  $n = N + L + 1$ . Various recursion relations of these functions, which are needed for our calculations, are given in Appendix B.

Our basis set finally reads

$$|\Pi\rangle = |N, L; (I, S_h), J; F, S_e; F_t, M_{F_t}\rangle \quad (23)$$

and we make the ansatz

$$|\Psi\rangle = \sum_{NLJFF_tM_{F_t}} c_{NLJFF_tM_{F_t}} |\Pi\rangle \quad (24)$$

with real coefficients  $c$ . Since the functions  $U_{NL}(r)$  actually depend on the coordinate  $\rho = r/\alpha$ , we substitute  $r \rightarrow \rho\alpha$  in the Hamiltonian (12) and multiply the corresponding Schrödinger equation  $H\Psi = E\Psi$  by  $\alpha^2$ . Then we calculate a matrix representation of the Schrödinger equation, which yields a generalized eigenvalue problem of the form

$$\mathbf{A}\mathbf{c} = E\mathbf{M}\mathbf{c}, \quad (25)$$

which is solved in atomic units using an appropriate LAPACK routine [40]. The matrix elements which enter the symmetric matrices  $\mathbf{A}$  and  $\mathbf{M}$  are given in Appendices C and D. The vector  $\mathbf{c}$  contains the coefficients of the ansatz (24). Since the basis cannot be infinitely large, the values of the quantum numbers are chosen in the following way: For each value of  $n = N + L + 1$  we use

$$\begin{aligned} L &= 0, \dots, n-1, \\ J &= 1/2, 3/2, \\ F &= |L - J|, \dots, \min(L + J, F_{\max}), \\ F_t &= F - 1/2, F + 1/2, \\ M_{F_t} &= -F_t, \dots, F_t. \end{aligned} \quad (26)$$

The value  $F_{\max}$  and the maximum value of  $n$  are chosen appropriately large so that the eigenvalues converge. Additionally, we can use the scaling parameter  $\alpha$  to enhance convergence. In particular, if the eigenvalues of excitonic states with principal quantum number  $n$  are calculated, we set  $\alpha = na_{\text{exc}}$  according to Ref. [39].

#### D. Oscillator strengths

If no external fields are present, the different terms of the Hamiltonian couple only basis states with even or with odd values of  $L$  (see Appendix C). Since we restrict ourselves to odd values of  $L$ , the exchange interaction and central-cell corrections can be neglected.

$F$  as well as  $M_F$  are good quantum numbers in the spherical approximation. In this case the usage of the total momentum  $F_t$  in our basis (23) seems unnecessary. However, we still keep the total momentum since it allows us to determine the symmetry of the different excitonic states.

If the spins of the electron and the hole are considered in the simple-band model, the exciton states are either spin-singlet or spin-triplet states. Since the spin is conserved in dipole transitions, the oscillator strength is nonzero only for the singlet states. However, an optical excitation at the  $\Gamma$ -point ( $\mathbf{k} = \mathbf{0}$ ) is forbidden in  $\text{Cu}_2\text{O}$  since the valence band and the conduction band have the same parity. Only  $\mathbf{k}$ -dependent admixtures to the transition matrix element enable an optical excitation. The leading term in this matrix element is therefore proportional to the  $\mathbf{k}$ -vector in Fourier space or to the gradient (of the envelope function) in position space at  $r = 0$ . As the  $\mathbf{k}$ -vector transforms according to the irreducible representation  $D^1$  of the rotation group, the envelope function of the exciton has to transform according to the same representation. Since  $L$  is a good quantum number in the simple-band model, only  $P$ -excitons, i.e., excitons with  $L = 1$ , are dipole-allowed in this case [16].

The oscillator strength is then nonzero only if the total symmetry of the exciton, which is given by the symmetry of envelope function and the symmetries of the bands,

$$\Gamma_{\text{exc}} = \Gamma_{\text{env}} \otimes \Gamma_c \otimes \Gamma_v, \quad (27)$$

is identical to the symmetry  $\Gamma_4^-$  of the dipole operator [3, 26].

Since we consider the symmetry of the valence band via the spins  $I$  and  $S_h$  as well as the symmetry of the conduction band via the spin  $S_e$  in our basis, the total symmetry of the exciton can immediately be obtained by an examination of the solutions of the Schrödinger equation in the complete basis set of Eq. (23). Three important points have to be considered in this examination:

We already stated in Sec. II C that it is possible to combine the different states  $|A, M_A\rangle$  of an arbitrary momentum  $A \leq 4$  to the states  $|A, \Gamma_i\rangle$ . Solving the eigenvalue problem (25), we obtain the coefficients  $c$  of the basis functions according to Eq. (24). We can now compare the coefficients of those basis functions with a fixed value of  $F_t \leq 4$  to the coefficients of the functions  $|A, \Gamma_i\rangle$  given in Ref. [26] to obtain the symmetry of the eigenstates.

If an eigenvalue is  $p$ -fold degenerate, one has to form appropriate linear combinations of the  $p$  eigenvectors  $\mathbf{c}$  at first, before a comparison with the coefficients of the states  $|A, \Gamma_i\rangle$  is possible.

The quasi-spin  $I$  transforms according to  $\Gamma_5^+$  whereas a normal spin one transforms according to  $\Gamma_4^+$ . Since  $\Gamma_5^+ = \Gamma_2^+ \otimes \Gamma_4^+$  holds for the cubic group  $O_h$  [26], one has to multiply the symmetries  $\Gamma_i$  obtained via the above comparison by  $\Gamma_2^+$  [20].

For the states of  $\Gamma_4^-$ -symmetry we can then calculate relative oscillator strengths: With the above explanations, the dipole-allowed states must have a nonvanishing overlap with the state [26]

$$\begin{aligned} |D\rangle = \frac{1}{\sqrt{2}} & \left( \left| \left( \frac{1}{2}, \frac{1}{2} \right) 0, 1; 1, 1; 2, 2 \right\rangle \right. \\ & \left. - \left| \left( \frac{1}{2}, \frac{1}{2} \right) 0, 1; 1, 1; 2, -2 \right\rangle \right), \end{aligned} \quad (28)$$

where the quantum numbers denote the angular momenta in  $|(S_e, S_h) S, I; I + S, L; F_t, M_{F_t}\rangle$ . This state transforms also according to the irreducible representation  $\Gamma_4^-$ . Its specific form shows that we assume the incident light to be linearly polarized [26]. The relative oscillator strengths are finally given by

$$f_{\text{rel}} \sim \left| \lim_{r \rightarrow 0} \frac{\partial}{\partial r} \langle D | \Psi(\mathbf{r}) \rangle \right|^2 \quad (29)$$

with the wave function of Eq. (24) in spatial representation (see Appendix A).

### III. RESULTS AND DISCUSSION

#### A. $F=5/2$ and $7/2$ excitonic lines of cuprous oxide

In this section we apply the method presented in Sec. II and repeat the analysis of Ref. [20]. Deviations from the results in Ref. [20] are observed and discussed. Using the parameters  $\Delta = 0.1338 \text{ eV}$ ,  $\gamma'_1 = 2.78$ ,  $\mu' = 0.47$  from Ref. [14], the parameter  $\delta'$  has been determined in Ref. [20] by comparing theoretical results with experimental absorption spectra.

In the spherical approximation  $F$  and  $M_F$  are good quantum numbers. Including the cubic part of the Hamiltonian  $H_d$ , the reduction of the irreducible representations  $D^F$  of the rotation group by the cubic group  $O_h$  has to be considered [26]. With the additional factor  $\Gamma_2^+$  as described in Sec. IID, we obtain for the symmetry of the envelope function and the hole

$$\tilde{D}^{\frac{1}{2}} = D^{\frac{1}{2}} \otimes \Gamma_2^+ = \Gamma_6^- \otimes \Gamma_2^+ = \Gamma_7^-, \quad (30a)$$

$$\tilde{D}^{\frac{3}{2}} = D^{\frac{3}{2}} \otimes \Gamma_2^+ = \Gamma_8^- \otimes \Gamma_2^+ = \Gamma_8^-, \quad (30b)$$

$$\begin{aligned} \tilde{D}^{\frac{5}{2}} &= D^{\frac{5}{2}} \otimes \Gamma_2^+ = (\Gamma_7^- \oplus \Gamma_8^-) \otimes \Gamma_2^+ \\ &= \Gamma_6^- \oplus \Gamma_8^-, \end{aligned} \quad (30c)$$

$$\begin{aligned} \tilde{D}^{\frac{7}{2}} &= D^{\frac{7}{2}} \otimes \Gamma_2^+ = (\Gamma_6^- \oplus \Gamma_7^- \oplus \Gamma_8^-) \otimes \Gamma_2^+ \\ &= \Gamma_7^- \oplus \Gamma_6^- \oplus \Gamma_8^-. \end{aligned} \quad (30d)$$

The Hamiltonian couples only states with even or odd values of  $L$ . Since in the simple-band model only states with  $L = 1$  are dipole-allowed, we only include states with odd values of  $L$  in our basis. This is the reason for the negative parities in Eqs. (30a)-(30d). Furthermore, we can neglect the central-cell corrections and the exchange interaction in the following since they only affect states with  $L = 0$ .

As can be seen from Eqs. (30c) and (30d) the states with  $F = 5/2$  and  $F = 7/2$  split into five states with the symmetries  $\Gamma_6^-$ ,  $\Gamma_7^-$ , and  $\Gamma_8^-$ . The degeneracies of these states are two for  $\Gamma_6^-$  and  $\Gamma_7^-$  and four for  $\Gamma_8^-$ . Including the symmetry  $\Gamma_6^+$  of the electron spin, we obtain

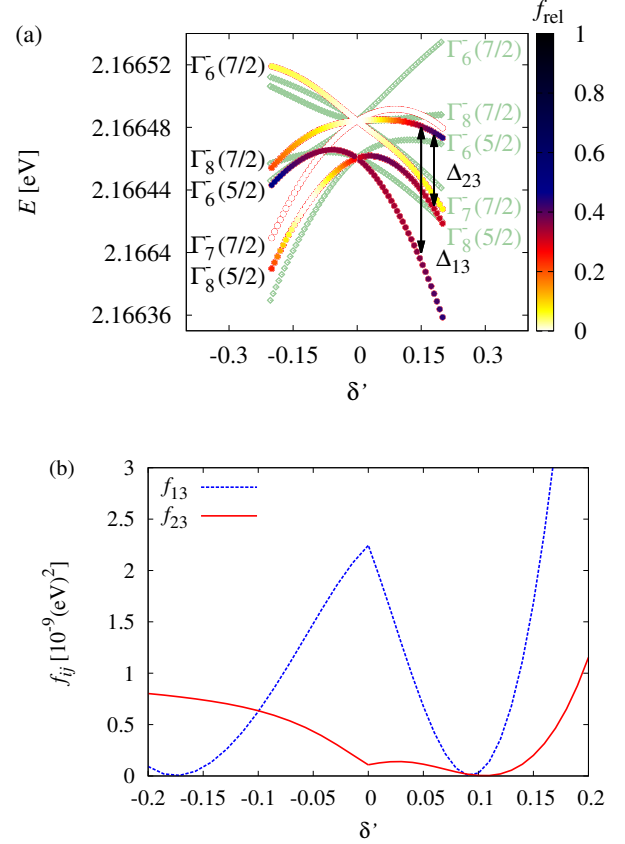


FIG. 2. (Color online) (a) Comparison of the results of Ref. [20] (green diamonds) and the results obtained by the method described in Sec. II (circles). The splitting of the  $F = 5/2$  and  $F = 7/2$  states due to the cubic part of the Hamiltonians is depicted for the principal quantum number  $n = 4$ . Our symmetry assignment (left) differs from the one of Ref. [20] (right). The color bar shows the relative oscillator strengths in arbitrary units. The state assigned with  $\Gamma_6^-(7/2)$  has only small oscillator strength. The parameters  $\Delta_{13}$  and  $\Delta_{23}$  denote the line spacings between the remaining dipole-allowed states. (b) The functions  $f_{13}(\delta')$  and  $f_{23}(\delta')$  as defined in Eq. (32). The value  $\delta' \approx 0.1$ , for which both function values are minimal, is the value of this material parameter in  $\text{Cu}_2\text{O}$  if  $\mu' = 0.47$  and  $\eta_i = 0$  holds. The kinks at  $\delta' = 0$  are due to the definition of the quantities  $\Delta_{13}$  and  $\Delta_{23}$ . For further information see text.

the symmetry of the exciton and can determine which of these states are dipole-allowed, viz.,

$$\Gamma_6^- \otimes \Gamma_6^+ = \Gamma_1^- \oplus \Gamma_4^-, \quad (31a)$$

$$\Gamma_7^- \otimes \Gamma_6^+ = \Gamma_2^- \oplus \Gamma_5^-, \quad (31b)$$

$$\Gamma_8^- \otimes \Gamma_6^+ = \Gamma_3^- \oplus \Gamma_4^- \oplus \Gamma_5^-. \quad (31c)$$

Since only the threefold degenerate states of symmetry  $\Gamma_4^-$  are dipole-allowed, four lines are visible in experiments at the most. However, in Ref. [20] only three lines



could be observed.

We solve the generalized eigenvalue problem (25) in the complete basis of Eq. (23) with the additional quantum number  $F_t$ , determine the states of symmetry  $\Gamma_4^-$ , and calculate the oscillator strengths. Even though the states with  $F = 5/2$  and  $F = 7/2$  lie energetically very close together in the spherical approximation, it is inappropriate to consider only basis functions with these two values of  $F$  in our ansatz. Including all states with  $F \leq 15/2$ , we obtain a clearly different result in comparison to the one of Ref. [20]. In Fig. 2(a) we depict the results of Ref. [20] for the principal quantum number  $n = 4$  by green diamonds and our results by circles. For the  $9j$ -symbol in Eq. (C7) we use the relations given in Refs. [36, 41], so that our result differs by an exchange of the first two rows in the  $9j$ -symbol of Eq. (14) of Ref. [20] or of Eq. (A2) of Ref. [11]. We are convinced that the formulas given in Refs. [36, 41] are correct as the quantum numbers in the rows of the  $9j$ -symbol appear in the same order as they appear in our basis states. An odd permutation of rows can lead to a change in the sign of the  $9j$ -symbol depending on the quantum numbers included [36] (cf. also Appendix C). Therefore, our assignment of the lines with the symmetries  $\Gamma_6^-$ ,  $\Gamma_7^-$ ,  $\Gamma_8^-$  in Fig. 2(a) differs from the one of Ref. [20]. The oscillator strengths of the states calculated are also depicted in this figure.

In Ref. [20] it has been discussed that also components of the order  $\mathbf{p}^4$  should be included in the Hamiltonian to obtain more reliable values for the oscillator strengths. However, the effect of these terms is considered to be very weak for the states investigated here and is generally only important for the  $1S$  exciton state [35]. Indeed, the effect of  $\mathbf{p}^4$ -terms significantly decreases with increasing principal quantum number  $n$  but a corresponding decrease of the oscillator strength between the  $n = 4$  states and the  $n = 5$  states cannot be observed experimentally [20]. This shows that an effect of  $\mathbf{p}^4$ -terms is not present at all. We therefore neglect these higher order terms in  $\mathbf{p}$ .

In Fig. 2(a) the state assigned with  $\Gamma_6^-$  ( $7/2$ ) has only small oscillator strength, which validates the fact that only three lines can be observed experimentally in absorption spectra. Furthermore, the two lines assigned with  $\Gamma_6^-$  ( $7/2$ ) and  $\Gamma_8^-$  ( $5/2$ ) could hardly be resolved in experiments for  $\delta' \geq 0.1$ .

In order to determine the correct value of  $\delta'$  we consider the energetic spacing between the lines. We use the same nomenclature as in Ref. [20]; i.e., the spacing between the state with the highest energy and the state with the lowest energy is called  $\Delta_{13}$  while the spacing between the state with the highest energy and the state with the second highest energy is called  $\Delta_{23}$  [see Fig. 2(a)]. Note that, e.g., the state with the lowest energy is  $\Gamma_8^-$  ( $5/2$ ) for  $\delta' < 0$  and  $\Gamma_6^-$  ( $5/2$ ) for  $\delta' > 0$  so that there are different lines entering  $\Delta_{13}$  and  $\Delta_{23}$  depending on  $\delta'$ . Since the spacings depend on the value of  $\delta'$  and the principal quantum number  $n$ , we use the notation  $\Delta_{ij}(\delta', n)$ .

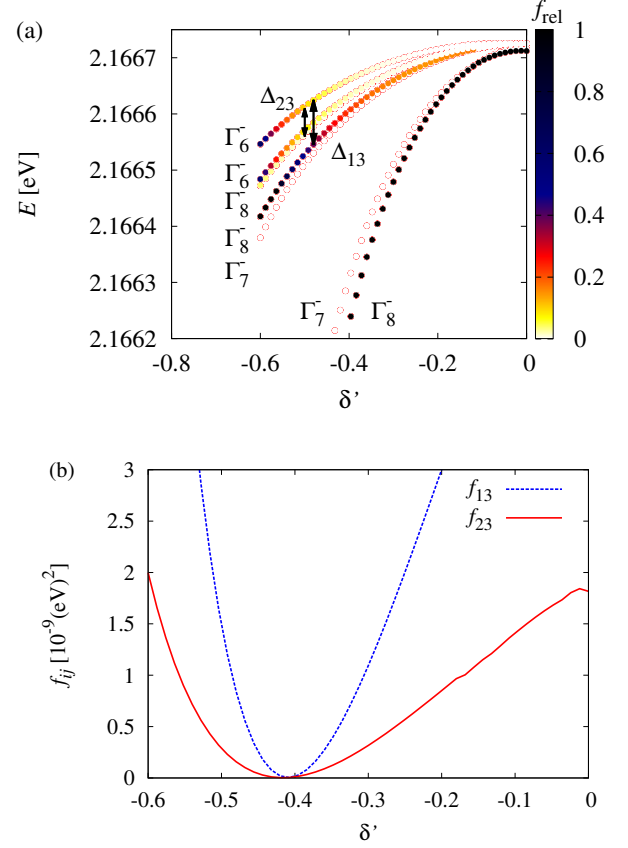


FIG. 3. (Color online) Same calculation as in Fig. 2 but for the material parameters  $\Delta$ ,  $\gamma_1'$ ,  $\mu'$ , and  $\epsilon_{\text{ta}i}$  obtained from band structure calculations [8, 30] (cf. Table I). (a) Relative oscillator strengths (color bar) of the exciton states with  $n = 4$  in arbitrary units. The assignment of  $F$  quantum numbers is omitted (see text). (b) The functions  $f_{13}(\delta')$  and  $f_{23}(\delta')$  as defined in Eq. (32). The optimum value for  $\delta'$  is here  $\delta' = -0.408$ . For further information see text.

Minimizing the functions

$$f_{ij}(\delta') = \sum_{n=4}^8 (\Delta_{ij}(\delta', n) - \Delta_{ij}^{\text{exp}}(n))^2, \quad (32)$$

where  $\Delta_{ij}^{\text{exp}}(n)$  denote the spacings in the experimental absorption spectrum, we obtain almost the same value of  $\delta'$  irrespective of the indices  $ij$  as can be seen from Fig. 2(b). The final value is

$$\delta' = 0.1, \quad (33)$$

which is clearly different from the value  $\delta' = -0.1$  of Ref. [20].

Even though the values  $\mu' = 0.47$  and  $\delta' = 0.1$  reproduce the experimental results of excitonic absorption spectra very well, we cannot disregard that these values originate from the valence band structure of  $\text{Cu}_2\text{O}$ . In Ref. [20] it has already been noted that a negative value of  $\delta'$  is expected due to a comparison with band structure



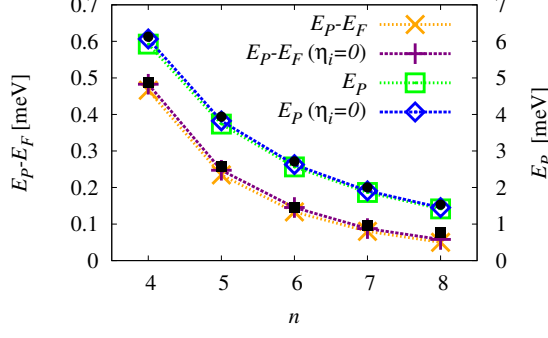


FIG. 4. (Color online) Binding energies  $E_P$  of the dipole-allowed  $P$  excitons and the energy difference between these excitons and the average energy of the dipole-allowed  $F$  excitons. Black dots and circles denote experimental data. Theoretical results are depicted by lines with points. The best agreement between theory and experiment is obtained for  $\delta' \approx -0.42$ . Without the  $\eta_i$ -dependent terms of Eq. (6) an even better agreement can be obtained for  $\delta' = -0.408$ .

calculations [30]. However, our calculations do not provide a negative value even if we include the state assigned with  $\Gamma_6^-$  (7/2) in our calculations.

A fit to band structure calculations yields [8]  $\mu' = 0.0586$  and  $\delta' = -0.404$  as already mentioned in Sec. II B. These values are clearly different from the results of the above calculation. Therefore, we assume that there is more than one combination of the parameters  $\mu'$  and  $\delta'$  yielding the correct spacings between the observed exciton states.

To prove our assumption, we perform the same analysis again, using the parameters  $\Delta = 0.131$  eV,  $\gamma'_1 = 2.77$ , and  $\mu' = 0.0586$  as given values. We now also include the terms with the coefficients  $\eta_i$  of the Hamiltonian (6) of the hole. We restrict the analysis to negative values of  $\delta'$ . The results are depicted in Fig. 3. Note that the value of  $\mu' = 0.0586$  is so small that the states with different quantum number  $F$  are hardly separated for  $\delta' = 0$ . Since these states mix for finite  $\delta'$  it is therefore inappropriate to give the symmetries of the states in the form  $\Gamma_i^-(F)$  and we omit the assignment with  $F$ . Further-

more, the spacing between the lower lying  $\Gamma_6^-$  state and the higher lying  $\Gamma_8^-$  state, which has a very small oscillator strength, is so small that it can hardly be resolved in experiments. This proves again that there are only three lines observable in experiments. Our calculations yield

$$\delta' = -0.408, \quad (34)$$

which is in excellent agreement with the expected value of  $\delta' = -0.404$ .

In Fig. 4 we depict the binding energies  $E_P$  of the dipole-allowed  $P$  excitons as well as the energy difference between these excitons and the average energy of the dipole-allowed  $F$  excitons. We use the nomenclature of Ref. [20] so that the  $P$  excitons are the energetically lower lying states of symmetry  $\Gamma_7^-$  and  $\Gamma_8^-$  in Fig. 3(a) whereas the  $F$  excitons are the remaining states in this Figure. We obtain a good agreement between theory and experiment for a slightly different value of  $\delta' \approx -0.42$ .

Small uncertainties in the material parameters still remain but can be explained in terms of some approximations made, e.g., the parameters  $A_i$  and  $B_i$  taken from Ref. [8] are fit parameters to band structure calculations and are hence afflicted with errors. Another influence on the exciton spectrum are phonons [18], which our theory does not account for and which also make an experimental determination of the correct position of exciton resonances difficult [16]. Finally, we think that out of the several combinations of  $\mu'$  and  $\delta'$ , which reproduce the exciton spectrum, the parameters obtained from band structure calculations are the correct ones to describe this spectrum.

## B. $K$ -dependent line splitting

In this section we discuss the  $K$ -dependent line splitting observed in Ref. [42] in terms of the complex valence band structure of  $\text{Cu}_2\text{O}$ . The Hamiltonian (7) depends only on the relative coordinate  $\mathbf{r} = \mathbf{r}_e - \mathbf{r}_h$  of electron and hole. For this reason the momentum of the center of mass  $\hbar\mathbf{K}$  is a constant of motion [43]. About ten years ago the  $K$ -dependent line splitting of the  $1S$  exciton state was observed and explained in terms of a  $K$ -dependent short-range exchange interaction of the form [23, 24, 42]

$$J(\mathbf{K}) = \Delta_1 \begin{pmatrix} K^2 & 0 & 0 \\ 0 & K^2 & 0 \\ 0 & 0 & K^2 \end{pmatrix} + \Delta_3 \begin{pmatrix} 3K_1^2 - K^2 & 0 & 0 \\ 0 & 3K_2^2 - K^2 & 0 \\ 0 & 0 & 3K_3^2 - K^2 \end{pmatrix} + \Delta_5 \begin{pmatrix} 0 & K_1K_2 & K_1K_3 \\ K_1K_2 & 0 & K_2K_3 \\ K_1K_3 & K_2K_3 & 0 \end{pmatrix}, \quad (35)$$

Fitting this ansatz to experimental spectra of the  $1S$  exciton yielded

$$\Delta_1 = -8.6 \mu\text{eV}, \quad \Delta_3 = -1.3 \mu\text{eV}, \quad \Delta_5 = 2 \mu\text{eV}. \quad (36)$$

However, it has been reported that a  $K$ -dependent short-range exchange interaction is far too small to cause the large line splitting observed [35].

As has already been stated in Sec. II A, when considering the ortho exciton states each of these states can have a larger contribution of one of the orbital Bloch functions  $xy$ ,  $yz$ , or  $zx$  without a violation of symmetry, respectively. However, if one orbital Bloch component predominates, the anisotropic dispersion of the Bloch function will lead to an anisotropic dispersion of the excitons. Thus, the  $K$ -dependent line splitting of the ortho exciton observed in Refs. [23, 24, 42] should be a direct consequence of the disparity in the orbital Bloch components of this exciton. Therefore, we think that the  $I$ -dependent terms in Eq. (7) are the reason for this splitting and we will show that these terms are of the same form as the ones in Eq. (35). Since  $\eta_i \ll \gamma_i$  holds in Eq. (6), we set  $\eta_i = 0$  in the following.

Inserting the well-known coordinates and momenta of relative and center of mass motion,

$$\mathbf{r} = \mathbf{r}_e - \mathbf{r}_h, \quad (37a)$$

$$\mathbf{R} = (m_e \mathbf{r}_e + m_h \mathbf{r}_h) / (m_e + m_h), \quad (37b)$$

$$\mathbf{p} = (m_h \mathbf{p}_e - m_e \mathbf{p}_h) / (m_e + m_h), \quad (37c)$$

$$\mathbf{P} = \mathbf{p}_e + \mathbf{p}_h = \hbar \mathbf{K}, \quad (37d)$$

in Eq. (7) leads to a coupling term between these motions in the kinetic energy [38, 43]:

$$H = T_r(\mathbf{p}) + T_c(\mathbf{p}, \mathbf{K}) + T_t(\mathbf{K}) + V(\mathbf{r}). \quad (38)$$

In Ref. [43] a different transformation of coordinates was proposed, by which the coupling term  $T_c$  vanishes. This

transformation reads

$$(\mathbf{p}_h)_i = \sum_j \mathbf{A}_{ij} K_j - p_i, \quad (39a)$$

$$(\mathbf{p}_e)_i = \sum_j (\hbar \delta_{ij} \mathbf{1} - \mathbf{A}_{ij}) K_j + p_i, \quad (39b)$$

where the terms  $\mathbf{A}_{ij}$  are assumed to be spin matrices. However, in the calculations of Ref. [43] the spin-orbit coupling was assumed to be infinitely large so that only states with  $J = 3/2$  were considered. We will now calculate the appropriate matrices  $\mathbf{A}_{ij}$  for the Hamiltonian (7) and compare the resulting expression for  $T_t(\mathbf{K})$  with the ansatz for the exchange interaction in Refs. [23, 24, 42].

We define the matrices

$$\mathbf{I}_{ij} = 3 \{ \mathbf{I}_i, \mathbf{I}_j \} - 2\hbar^2 \delta_{ij} \mathbf{1} \quad (40)$$

according to [12] and note that these operators form a closed subset with respect to the symmetric product  $\{a, b\} = \frac{1}{2}(ab + ba)$  (see Appendix E). Therefore, we make the ansatz

$$\mathbf{A}_{jj} = \hbar^2 C_1 \mathbf{1} + \frac{1}{3} C_2 \mathbf{I}_{jj} + \frac{1}{3} C_3 \mathbf{I}_{kl}, \quad (41a)$$

$$\mathbf{A}_{jk} = \hbar^2 C_4 \mathbf{1} + \frac{1}{3} C_5 \mathbf{I}_{jk} + \frac{1}{3} C_6 \mathbf{I}_{ll}, \quad (41b)$$

with  $j \neq l \neq k \neq j$ , which respects the cubic symmetry of the solid. Inserting Eqs. (39a) and (39b) into the kinetic part of Eq. (7) and setting the coupling term  $T_c = 0$ , we can determine the coefficients  $C_i$ . The  $K$ -dependent part of the kinetic energy is then exactly of the same form as the exchange interaction terms in Refs. [23, 24, 42]:

$$T_t(\mathbf{K}) = \Omega_1 K^2 \mathbf{1} - \frac{\Omega_3}{\hbar^2} (K_1^2 \mathbf{I}_{11} + \text{c.p.}) - \frac{2\Omega_5}{3\hbar^2} (K_1 K_2 \mathbf{I}_{12} + \text{c.p.}) \quad (42)$$

or

$$T_t(\mathbf{K}) = \Omega_1 \begin{pmatrix} K^2 & 0 & 0 \\ 0 & K^2 & 0 \\ 0 & 0 & K^2 \end{pmatrix} + \Omega_3 \begin{pmatrix} 3K_1^2 - K^2 & 0 & 0 \\ 0 & 3K_2^2 - K^2 & 0 \\ 0 & 0 & 3K_3^2 - K^2 \end{pmatrix} + \Omega_5 \begin{pmatrix} 0 & K_1 K_2 & K_1 K_3 \\ K_1 K_2 & 0 & K_2 K_3 \\ K_1 K_3 & K_2 K_3 & 0 \end{pmatrix}, \quad (43)$$

where  $K$  is now given in units of  $k_0 \approx 2.62 \text{ m}^{-1}$ , i.e., the value at the exciton-photon resonance [24]. The dependency of the coefficients  $C_i$  and  $\Omega_i$  on the Luttinger parameters is given in Appendix E.

Since our coefficients  $\Omega_i$  cannot be directly compared with the according coefficients  $\Delta_i$  in Refs. [23, 24, 42], we use a different symbol to illustrate this fact. The impossibility of a direct comparison arises due to three important facts:

First, the operator  $T_t(\mathbf{K})$  describes the kinetic energy related to the motion of the center of mass, whereas Eq. (35) only describes the “exchange interaction,” i.e., the interaction without the spherically symmetric part of the kinetic energy. Therefore, it is  $\Omega_1 \hat{=} \hbar^2 K^2 / (2M) + \Delta_1$ ,  $\Omega_3 \hat{=} \Delta_3$ , and  $\Omega_5 \hat{=} \Delta_5$  with the exciton mass of the simple-band model  $M = m_e + m_h \approx 1.64 m_0$ .

Furthermore, the central-cell corrections apply for the  $1S$  exciton. However, the calculations on these corrections have been done within the simple band model and

the coefficients  $c_e = 1.35$ ,  $c_h = 1.35$  and  $d = 0.18$ , which have been introduced in Sec. II B, were obtained by comparing results to experimental data. Effects due to the complex valence band structure may therefore be already included in these central-cell corrections so that we cannot separate the true central-cell effects from the effects due to  $T_t(\mathbf{K})$ .

Finally, since the coefficients  $\Delta_i$  were obtained from experimental data, we have to consider that the  $K$ -dependent splitting is also influenced by the binding energy of the exciton. Therefore,  $T_t(\mathbf{K})$  has to either be included in the matrix diagonalization or at least be treated within perturbation theory as was done in Ref. [43].

However, Fig. 5 shows that there are significant changes in the values of the coefficients  $\Omega_3$  and  $\Omega_5$  if the parameters  $\mu'$  and  $\delta'$  are only slightly varied from  $\mu' = 0.0586$  and  $\delta' = -0.404$ . Consequently, a more comprehensive analysis of  $T_t(\mathbf{K})$  would not give more reliable results due to the small uncertainties in  $\mu'$  and  $\delta'$ , which have been discussed at the end of Sec. III A.

Therefore, we present only a very simple analysis of  $T_t(\mathbf{K})$ : Using  $\gamma'_1 = 2.77$  as a given value, we solve the equations

$$-1.3 \text{ } \mu\text{eV} = \Omega_3(\mu', \delta'), \quad (44a)$$

$$2.0 \text{ } \mu\text{eV} = \Omega_5(\mu', \delta') \quad (44b)$$

for  $\mu'$  and  $\delta'$  and obtain  $\mu' \approx 0.0583$  and  $\delta' \approx -0.442$ . Inserting these results in  $\Omega_1(\mu', \delta')$  yields  $\Omega_1 \approx 2.15 \text{ } \mu\text{eV}$  or  $\Omega_1 - \hbar^2 K^2 / (2M) \approx -13.73 \text{ } \mu\text{eV}$ . Of course, the deviation from the experimental value  $\Delta_1 = -8.6 \text{ } \mu\text{eV}$  could now be explained in terms of the simplicity of this analysis.

However, we have proved that there is clear evidence that the valence band structure or the term  $T_t(\mathbf{K})$  describing the kinetic energy of the motion of the center of mass of the exciton is the cause for the  $K$ -dependent behavior of the  $1S$  exciton observed in Refs. [23, 24, 42], whereas a  $K$ -dependent short-range interaction can most likely be excluded [35].

#### IV. SUMMARY AND OUTLOOK

Using the method of solving the Schrödinger equation in a complete basis, we determined the eigenstates of the cubic Hamiltonian of excitons accounting for the complex band structure. An evaluation of the calculated line spacings and oscillator strengths proved that there are several combinations of the parameters  $\mu'$  and  $\delta'$  by which the excitonic spectra can be described. However, we assume that the values resulting from band structure calculations are the correct ones. Using the values  $\gamma'_1 = 2.77$ ,  $\mu' = 0.0586$ , and  $\delta' = -0.404$ , the Luttinger parameters of  $\text{Cu}_2\text{O}$  are

$$\gamma_1 = 1.76, \quad \gamma_2 \approx 0.75, \quad \gamma_3 \approx -0.37. \quad (45)$$

Furthermore, we separated the relative motion and the motion of the center of mass using an appropriate coordinate transformation. The final result allows us to

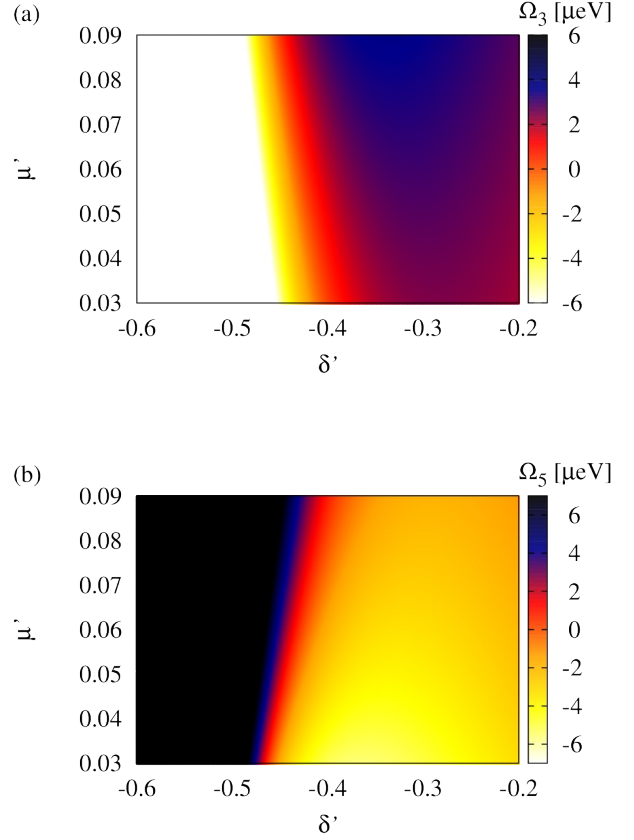


FIG. 5. (Color online) The values of the coefficients (a)  $\Omega_3$  and (b)  $\Omega_5$  as functions of  $\mu'$  and  $\delta'$ .

explain the  $K$ -dependent line splitting of the  $1S$  exciton state in terms of the complex kinetic energy of the motion of the center of mass. As a next step, we plan to extend our method to calculate excitonic spectra of  $\text{Cu}_2\text{O}$  in the presence of external magnetic and electric fields.

#### ACKNOWLEDGMENTS

We thank M. M. Glazov, M. A. Semina, D. Fröhlich, M. Bayer and H. Cartarius for helpful discussions.

#### Appendix A: Oscillator strengths

We now give the formula for the relative oscillator strength (see Sec. II D)

$$f_{\text{rel}} \sim \left| \lim_{r \rightarrow 0} \frac{\partial}{\partial r} \langle D | \Psi(\mathbf{r}) \rangle \right|^2. \quad (A1)$$

Using the wave function of Eq. (24), we find

$$\begin{aligned}
f_{\text{rel}} \sim & \left| \sum_{N J F F_t} \sum_{M_{S_e} M_I} \sum_{k=\pm 2} c_{N1 J F F_t k} \right. \\
& \times k (-1)^{F-J-3M_{S_e}-M_I+\frac{3}{2}} [(N+1)(N+3)]^{\frac{1}{2}} \\
& \times [(2J+1)(2F+1)(2F_t+1)]^{\frac{1}{2}} \\
& \times \begin{pmatrix} 1 & \frac{1}{2} & J \\ M_I & -M_{S_e} & M_{S_e} - M_I \end{pmatrix} \\
& \times \begin{pmatrix} 1 & 1 & 2 \\ M_I & k - M_I & -k \end{pmatrix} \\
& \times \begin{pmatrix} F & \frac{1}{2} & F_t \\ k - M_{S_e} & M_{S_e} & -k \end{pmatrix} \\
& \left. \times \begin{pmatrix} 1 & J & F \\ k - M_I & M_I - M_{S_e} & M_{S_e} - k \end{pmatrix} \right|^2. \quad (\text{A2})
\end{aligned}$$

### Appendix B: Recursion relations of the Coulomb-Sturmian functions

In this section we give all important recursion relations of the Coulomb-Sturmian functions based on the calculations in Ref. [44]. In this regard, we also give the recursion relations needed if external magnetic or electric fields are present. The Coulomb-Sturmian functions read

$$\begin{aligned}
\phi_{N,L,M}(\mathbf{r}) &= U_{NL}(\rho) Y_{LM}(\Omega) \\
&= N_{NL} (2\rho)^L e^{-\rho} L_N^{2L+1}(2\rho) Y_{LM}(\Omega) \quad (\text{B1})
\end{aligned}$$

with  $\rho = r/\alpha$ , a normalization factor

$$N_{NL} = \frac{2}{\sqrt{\alpha^3}} \left[ \frac{N!}{(N+2L+1)!(N+L+1)} \right]^{\frac{1}{2}}, \quad (\text{B2})$$

the associated Laguerre polynomials  $L_n^m(x)$ , and an arbitrary scaling parameter  $\alpha$ . The radial functions obey the orthogonality relation

$$\int_0^\infty dr r U_{N'L}(r) U_{NL}(r) = \frac{1}{\alpha(N+L+1)} \delta_{NN'}. \quad (\text{B3})$$

For the recursion relations we set  $\alpha = 1$  and omit the dependency of the functions  $\phi_{N,L,M}$  on  $\mathbf{r}$ . Coefficients in these relations will be given, e.g., in the form  $(R_1)_{NL}^j$ , which means that they are functions of  $j$ ,  $n$ , and  $L$ , etc. The vectors  $\hat{n}$  and  $\nabla^{\hat{n}}$  are defined as in Ref. [44].

$$\hat{n}_3 \phi_{N,L,M} = \sum_{j=\pm 1} (N_1)_{LM}^j \phi_{N,L+j,M} \quad (\text{B4})$$

$$\begin{aligned}
(N_1)_{LM}^j &= \delta_{1j} \left\{ \left[ \frac{(L+M+1)(L-M+1)}{(2L+1)(2L+3)} \right]^{\frac{1}{2}} \right\} \\
&+ \delta_{-1j} \left\{ \left[ \frac{(L+M)(L-M)}{(2L+1)(2L-1)} \right]^{\frac{1}{2}} \right\} \quad (\text{B5})
\end{aligned}$$

$$\nabla_3^{\hat{n}} \phi_{N,L,M} = \sum_{j=\pm 1} (D_1)_{LM}^j \phi_{N,L+j,M} \quad (\text{B6})$$

$$\begin{aligned}
(D_1)_{LM}^j &= \delta_{1j} \left\{ -L (N_1)_{LM}^1 \right\} \\
&+ \delta_{-1j} \left\{ (L+1) (N_1)_{LM}^{-1} \right\} \quad (\text{B7})
\end{aligned}$$

$$r \phi_{N,L,M} = \sum_{j=-1}^1 (R_1)_{NL}^j \phi_{N+j,L,M} \quad (\text{B8})$$

$$\begin{aligned}
(R_1)_{NL}^j &= \delta_{1j} \left\{ -\frac{1}{2} [(N+1)(N+L+2)]^{\frac{1}{2}} \right. \\
&\quad \times \left[ \frac{(N+2L+2)}{(N+L+1)} \right]^{\frac{1}{2}} \left. \right\} \\
&+ \delta_{0j} \{ N+L+1 \} \\
&+ \delta_{-1j} \left\{ -\frac{1}{2} [(N)(N+L)]^{\frac{1}{2}} \right. \\
&\quad \times \left[ \frac{(N+2L+1)}{(N+L+1)} \right]^{\frac{1}{2}} \left. \right\} \quad (\text{B9})
\end{aligned}$$

$$r \frac{\partial}{\partial r} \phi_{N,L,M} = \sum_{j=-1}^{-1} (RP_1)_{NL}^j \phi_{N+j,L,M} \quad (\text{B10})$$

$$\begin{aligned}
(RP_1)_{NL}^j &= \delta_{-1j} \left\{ (R_1)_{NL}^{-1} \right\} \\
&+ \delta_{0j} \{ -1 \} + \delta_{1j} \left\{ - (R_1)_{NL}^1 \right\} \quad (\text{B11})
\end{aligned}$$

$$\begin{aligned}
r \phi_{N,L,M} &= \sum_{j=-2}^0 (L_1)_{NL}^{j1} \phi_{N+j,L+1,M} \\
&= \sum_{j=0}^2 (L_1)_{NL}^{j-1} \phi_{N+j,L-1,M} \quad (\text{B12})
\end{aligned}$$

$$\begin{aligned}
(L_1)_{NL}^{jk} &= \delta_{2j}\delta_{-1k} \left\{ \frac{1}{2} [(N+2)(N+1)]^{\frac{1}{2}} \right. \\
&\quad \times \left[ \frac{(N+L+2)}{(N+L+1)} \right]^{\frac{1}{2}} \Big\} \\
&+ \delta_{1j}\delta_{-1k} \left\{ -[(N+1)(N+2L+1)]^{\frac{1}{2}} \right\} \\
&+ \delta_{0j}\delta_{-1k} \left\{ \frac{1}{2} [(N+2L)(N+2L+1)]^{\frac{1}{2}} \right. \\
&\quad \times \left[ \frac{(N+L)}{(N+L+1)} \right]^{\frac{1}{2}} \Big\} \\
&+ \delta_{0j}\delta_{1k} \left\{ \frac{1}{2} [(N+2L+2)(N+2L+3)]^{\frac{1}{2}} \right. \\
&\quad \times \left[ \frac{(N+L+2)}{(N+L+1)} \right]^{\frac{1}{2}} \Big\} \\
&+ \delta_{-1j}\delta_{1k} \left\{ -[(N)(N+2L+2)]^{\frac{1}{2}} \right\} \\
&+ \delta_{-2j}\delta_{1k} \left\{ \frac{1}{2} [(N)(N-1)]^{\frac{1}{2}} \right. \\
&\quad \times \left[ \frac{(N+L)}{(N+L+1)} \right]^{\frac{1}{2}} \Big\} \quad (B13)
\end{aligned}$$

With these relations we calculate combined formulas:

$$r^2\phi_{N,L,M} = \sum_{j=-2}^2 (R_2)_{NL}^j \phi_{N+j,L,M} \quad (B14)$$

$$(R_2)_{NL}^j = \sum_{w=j-1}^{j+1} (R_1)_{NL}^w (R_1)_{N+w,L}^{j-w} \quad (B15)$$

$$r^3\phi_{N,L,M} = \sum_{j=-3}^3 (R_3)_{NL}^j \phi_{N+j,L,M} \quad (B16)$$

$$(R_3)_{NL}^j = \sum_{w=j-1}^{j+1} (R_2)_{NL}^w (R_1)_{N+w,L}^{j-w} \quad (B17)$$

$$\begin{aligned}
r\hat{n}_3\phi_{N,L,M} &= \sum_{k=\pm 1} \sum_{j=-1-k}^{1-k} (LN_1)_{NLM}^{jk} \\
&\quad \times \phi_{N+j,L+k,M} \quad (B18)
\end{aligned}$$

$$(LN_1)_{NLM}^{jk} = (L_1)_{NL}^{jk} (N_1)_{LM}^k \quad (B19)$$

$$\begin{aligned}
r^2\hat{n}_3\phi_{N,L,M} &= \sum_{k=\pm 1} \sum_{j=-2-k}^{2-k} (RLN_1)_{NLM}^{jk} \\
&\quad \times \phi_{N+j,L+k,M} \quad (B20)
\end{aligned}$$

$$\begin{aligned}
(RLN_1)_{NLM}^{jk} &= \sum_{w=j-1}^{j+1} (LN_1)_{NLM}^{wk} \\
&\quad \times (R_1)_{N+w,L+k}^{j-w} \quad (B21)
\end{aligned}$$

$$\begin{aligned}
r^2\hat{n}_3^2\phi_{N,L,M} &= \sum_{k=0,\pm 2} \sum_{j=-2-k}^{2-k} (LN_2)_{NLM}^{jk} \\
&\quad \times \phi_{N+j,L+k,M} \quad (B22)
\end{aligned}$$

$$\begin{aligned}
(LN_2)_{NLM}^{jk} &= \sum_{v=\pm 1} \sum_{w=j-1-v}^{j+1-v} (LN_1)_{NLM}^{wk+v} \\
&\quad \times (LN_1)_{N+w,L+k+v}^{j-w-v} \quad (B23)
\end{aligned}$$

$$\begin{aligned}
r^3\hat{n}_3^2\phi_{N,L,M} &= \sum_{k=0,\pm 2} \sum_{j=-3-k}^{3-k} (R_1LN_2)_{NLM}^{jk} \\
&\quad \times \phi_{N+j,L+k,M} \quad (B24)
\end{aligned}$$

$$\begin{aligned}
(R_1LN_2)_{NLM}^{jk} &= \sum_{w=j-1}^{j+1} (LN_2)_{NLM}^{wk} \\
&\quad \times (R_1)_{N+w,L+k}^{j-w} \quad (B25)
\end{aligned}$$

$$r^2\frac{\partial}{\partial r}\phi_{N,L,M} = \sum_{j=-2}^2 (R_2P_1)_{NL}^j \phi_{N+j,L,M} \quad (B26)$$

$$(R_2P_1)_{NL}^j = \sum_{w=j-1}^{j+1} (RP_1)_{NL}^w (R_1)_{N+w,L}^{j-w} \quad (B27)$$

$$r^3 \frac{\partial}{\partial r} \phi_{N,L,M} = \sum_{j=-3}^3 (R_3 P_1)_{NL}^j \phi_{N+j,L,M} \quad (\text{B28})$$

$$(R_3 P_1)_{NL}^j = \sum_{w=j-1}^{j+1} (R_2 P_1)_{NL}^w (R_1)_{N+w,L}^{j-w} \quad (\text{B29})$$

### Appendix C: Matrix elements

In this section we give all matrix elements of the terms of the Hamiltonian  $H$  [Eq. 12] in the basis of Eq. (23) in Hartree units using the formalism of irreducible tensors [36]. We use the abbreviation

$$\tilde{\delta}_{\Pi\Pi'} = \delta_{LL'} \delta_{JJ'} \delta_{FF'} \delta_{F_t F'_t} \delta_{M_{F_t} M'_{F_t}} \quad (\text{C1})$$

in the following. The functions of the form  $(R_1)_{NL}^j$  are taken from the recursion relations of the Coulomb-Sturmian functions in Appendix B. The value of the integral  $I_{N' L'; NL}$  is given in Appendix D.

$$\langle \Pi' | r^{-1} | \Pi \rangle = \tilde{\delta}_{\Pi\Pi'} \delta_{NN'} [N + L + 1]^{-1} \quad (\text{C2})$$

$$\langle \Pi' | 1 | \Pi \rangle = \tilde{\delta}_{\Pi\Pi'} \sum_{j=-1}^1 (R_1)_{NL}^j [N + L + j + 1]^{-1} \delta_{N',N+j} \quad (\text{C3})$$

$$\langle \Pi' | p^2 | \Pi \rangle = 2\tilde{\delta}_{\Pi\Pi'} \delta_{NN'} - \tilde{\delta}_{\Pi\Pi'} \sum_{j=-1}^1 (R_1)_{NL}^j [N + L + j + 1]^{-1} \delta_{N',N+j} \quad (\text{C4})$$

$$\langle \Pi' | 1 + I^{(1)} \cdot S_{\text{h}}^{(1)} | \Pi \rangle = \tilde{\delta}_{\Pi\Pi'} \left( \frac{1}{2} J(J+1) - \frac{3}{8} \right) \sum_{j=-1}^1 (R_1)_{NL}^j [N + L + j + 1]^{-1} \delta_{N',N+j} \quad (\text{C5})$$

$$\langle \Pi' | P^{(2)} \cdot I^{(2)} | \Pi \rangle = \sqrt{5} \left\langle \Pi' \left| \left[ P^{(2)} \times I^{(2)} \right]_0^{(0)} \right| \Pi \right\rangle \quad (\text{C6})$$

$$\left\langle \Pi' \left| \left[ P^{(2)} \times I^{(2)} \right]_q^{(K)} \right| \Pi \right\rangle = 3\sqrt{5} (-1)^{F'_t + F_t - M'_{F_t} + F' + J + K} \left\langle N' L' \left\| P^{(2)} \right\| N L \right\rangle$$

$$\times [(2F_t + 1)(2F'_t + 1)(2F + 1)(2F' + 1)(2K + 1)(2J + 1)(2J' + 1)]^{\frac{1}{2}}$$

$$\times \begin{pmatrix} F'_t & K & F_t \\ -M'_{F_t} & q & M_{F_t} \end{pmatrix} \begin{Bmatrix} F' & F'_t & \frac{1}{2} \\ F_t & F & K \end{Bmatrix} \begin{Bmatrix} 1 & J' & \frac{1}{2} \\ J & 1 & 2 \end{Bmatrix} \begin{Bmatrix} L' & L & 2 \\ J' & J & 2 \\ F' & F & K \end{Bmatrix} \quad (\text{C7})$$

$$\langle \Pi' | p^2 (I^{(1)} \cdot S_{\text{h}}^{(1)}) | \Pi \rangle = \frac{1}{2} \left( J(J+1) - \frac{11}{4} \right) \langle \Pi' | p^2 | \Pi \rangle \quad (\text{C8})$$

$$\left\langle \Pi' \left| P^{(2)} \cdot \left[ I^{(2)} \times S_{\text{h}}^{(1)} \right]^{(2)} \right| \Pi \right\rangle = \sqrt{5} \left\langle \Pi' \left| \left[ P^{(2)} \times \left[ I^{(2)} \times S_{\text{h}}^{(1)} \right]^{(2)} \right]_0^{(0)} \right| \Pi \right\rangle \quad (\text{C9})$$

$$\begin{aligned}
\left\langle \Pi' \left| \left[ P^{(2)} \times \left[ I^{(2)} \times S_h^{(1)} \right]^{(2)} \right]_q^{(K)} \right| \Pi \right\rangle &= 3\sqrt{5} (-1)^{F'_t + F_t - M'_{F_t} + F' + K + \frac{1}{2}} \left\langle N L' \left\| P^{(2)} \right\| N L \right\rangle \\
&\times [(2F_t + 1)(2F'_t + 1)(2F + 1)(2F' + 1)(2K + 1)(2J + 1)(2J' + 1)]^{\frac{1}{2}} \\
&\times \begin{pmatrix} F'_t & K & F_t \\ -M'_{F_t} & q & M_{F_t} \end{pmatrix} \begin{Bmatrix} F' & F'_t & \frac{1}{2} \\ F_t & F & K \end{Bmatrix} \begin{Bmatrix} L' & L & 2 \\ J' & J & 2 \\ F' & F & K \end{Bmatrix} \begin{Bmatrix} 1 & 1 & 1 \\ \frac{1}{2} & \frac{1}{2} & 1 \\ J' & J & 2 \end{Bmatrix} \quad (C10)
\end{aligned}$$

In Eq. (C7) the order of the quantum numbers in the rows of the  $9j$ -symbol is given by relations in Refs. [36, 41] and differs from Eq. (14) of the Supplementary Material of Ref. [20] or Eq. (A2) of Ref. [11]. This odd permutation of rows changes the sign of the sign of the  $9j$ -symbol by [36]

$$(-1)^{L' + L + 2 + J' + J + 2 + F' + F + 4}. \quad (C11)$$

So there is change in the sign of the  $9j$ -symbol, e.g., for  $L = L' = 3$ ,  $J = 1/2$ ,  $J' = 3/2$  and  $F = F' = 5/2$  (cf. Eq. (15a) of the Supplementary Material of Ref. [20]).

---

#### Appendix D: Reduced matrix elements

We now give the value of the reduced matrix element  $\langle N' L' \left\| P^{(2)} \right\| N L \rangle$ . We use the abbreviation  $I_{N' L'; N L}$  for the integral

$$\begin{aligned}
I_{N' L'; N L} &= \int_0^\infty dr U_{N' L'}(r) U_{N L}(r) \\
&= 2 \left[ \frac{N'! N! (N' + 2L' + 1)! (N + 2L + 1)!}{(N' + L' + 1)! (N + L + 1)!} \right]^{\frac{1}{2}} \\
&\times \sum_{k=0}^{N'} \sum_{j=0}^N \frac{(k + j + L + L')!}{k! j! (N' - k)! (N - j)!} \\
&\times \frac{(-1)^{k+j}}{(k + 2L' + 1)! (j + 2L + 1)!} \quad (D1)
\end{aligned}$$

with  $\alpha = 1$ . The functions of the form  $(R_1)_{NL}^j$  are taken from the recursion relations of the Coulomb-Sturmian functions in Appendix B.



$$\begin{aligned}
\langle N' L' \| P^{(2)} \| N L \rangle &= \delta_{L', L+2} \frac{3}{2} \left[ \frac{(2L+4)(2L+2)}{(2L+3)} \right]^{\frac{1}{2}} \\
&\times \left[ \sum_{j=-2}^2 \left( -(R_2)_{NL}^j - \delta_{j0} L(2L+3) \right) I_{N' L+2; N+j L} \right. \\
&\quad \left. + \sum_{j=-1}^1 \left( (2L+3)(RP_1)_{NL}^j + 2(N+L+1)(R_1)_{NL}^j \right) I_{N' L+2; N+j L} \right] \\
&+ \delta_{L', L} \left( -\sqrt{3} \right) \left[ \frac{L(2L+1)(2L+2)}{(2L+3)(2L-1)} \right]^{\frac{1}{2}} \\
&\times \left[ 2\delta_{NN'} - \sum_{j=-1}^1 (R_1)_{NL}^j [N+L+j+1]^{-1} \delta_{N', N+j} \right] \\
&+ \delta_{L', L-2} \frac{3}{2} \left[ \frac{(2L)(2L-2)}{(2L-1)} \right]^{\frac{1}{2}} \\
&\times \left[ \sum_{j=-2}^2 \left( -(R_2)_{NL}^j + \delta_{j0} (1-L-2L^2) \right) I_{N' L-2; N+j L} \right. \\
&\quad \left. + \sum_{j=-1}^1 \left( (1-2L)(RP_1)_{NL}^j + 2(N+L+1)(R_1)_{NL}^j \right) I_{N' L-2; N+j L} \right] \quad (D2)
\end{aligned}$$

### Appendix E: The matrices $\mathbf{I}_{jk}$

In Sec. IIIB we introduced the matrices

$$\mathbf{I}_{ij} = 3 \{ \mathbf{I}_i, \mathbf{I}_j \} - 2\hbar^2 \delta_{ij} \mathbf{1}. \quad (E1)$$

We will shortly list the main properties of these matrices. The second-rank tensor with the components  $\mathbf{I}_{ij}$  is symmetric

$$\mathbf{I}_{ij} = \mathbf{I}_{ji} \quad (E2)$$

and traceless

$$\sum_{i=1}^3 \mathbf{I}_{ii} = \mathbf{0}. \quad (E3)$$

As already stated in Sec. IIIB the operators  $\mathbf{I}_{ij}$  form a closed subset with respect to the symmetric product  $\{a, b\} = \frac{1}{2}(ab + ba)$ :

$$\{ \mathbf{I}_{jj}, \mathbf{I}_{jj} \} = \hbar^2 (2\hbar^2 \mathbf{1} - \mathbf{I}_{jj}), \quad (E4a)$$

$$\{ \mathbf{I}_{jk}, \mathbf{I}_{jk} \} = -\frac{3\hbar^2}{4} (-2\hbar^2 \mathbf{1} + \mathbf{I}_{jj} + \mathbf{I}_{kk}), \quad (E4b)$$

$$\{ \mathbf{I}_{jj}, \mathbf{I}_{kk} \} = \hbar^2 (-\hbar^2 \mathbf{1} + \mathbf{I}_{jj} + \mathbf{I}_{kk}), \quad (E4c)$$

$$\{ \mathbf{I}_{jj}, \mathbf{I}_{jk} \} = -\frac{\hbar^2}{2} \mathbf{I}_{jk}, \quad (E4d)$$

$$\{ \mathbf{I}_{jk}, \mathbf{I}_{kl} \} = -\frac{3\hbar^2}{4} \mathbf{I}_{jl}, \quad (E4e)$$

$$\{ \mathbf{I}_{jj}, \mathbf{I}_{kl} \} = \hbar^2 \mathbf{I}_{kl}, \quad (E4f)$$

where  $j \neq l \neq k \neq j$ .

The matrices can also be expressed in terms of irreducible tensors [12]:

$$\mathbf{I}_{11} = \frac{1}{2} \left[ I_2^{(2)} + I_{-2}^{(2)} - \sqrt{\frac{2}{3}} I_0^{(2)} \right] \quad (E5a)$$

$$\mathbf{I}_{22} = -\frac{1}{2} \left[ I_2^{(2)} + I_{-2}^{(2)} + \sqrt{\frac{2}{3}} I_0^{(2)} \right] \quad (E5b)$$

$$\mathbf{I}_{33} = \sqrt{\frac{2}{3}} I_0^{(2)} \quad (E5c)$$

$$\mathbf{I}_{12} = -\frac{i}{2} \left[ I_2^{(2)} - I_{-2}^{(2)} \right] \quad (\text{E5d})$$

$$\mathbf{I}_{23} = \frac{i}{2} \left[ I_1^{(2)} + I_{-1}^{(2)} \right] \quad (\text{E5e})$$

$$\mathbf{I}_{31} = -\frac{1}{2} \left[ I_1^{(2)} - I_{-1}^{(2)} \right] \quad (\text{E5f})$$

Furthermore, we list the results for the coefficients  $C_i$  and the dependency of the parameters  $\Omega_i$  of Sec. III B on the Luttinger parameters. The coefficients read

$$C_1 = \Xi \cdot \left( 2\gamma_1'^2 + 4\gamma_2^2 - 3\gamma_3^2 + 6\gamma_1'\gamma_2 + 6\gamma_2\gamma_3 + 3\gamma_1'\gamma_3 \right) \quad (\text{E6a})$$

$$C_2 = 6\Xi \cdot \left( 2\gamma_2^2 - 3\gamma_3^2 + 2\gamma_1'\gamma_2 + 3\gamma_2\gamma_3 \right) \quad (\text{E6b})$$

$$C_5 = 12\Xi \cdot \left( \gamma_2\gamma_3 + \gamma_1'\gamma_3 \right) \quad (\text{E6c})$$

$$C_3 = C_4 = C_6 = 0 \quad (\text{E6d})$$

with

$$\Xi = \frac{m_0}{\hbar m_e} \left[ (\gamma_1' - 2\gamma_2)(\gamma_1' + 4\gamma_2) \times (2\gamma_1' + 2\gamma_2 + 3\gamma_3) - 27\gamma_1'\gamma_3^2 \right]^{-1} \quad (\text{E7})$$

The parameters  $\Omega_i$  are given by

$$\begin{aligned} \frac{\Omega_1}{k_0^2} &= \frac{\hbar^2}{2m_e} - \frac{\hbar^3}{m_e} C_1 \\ &\quad + \frac{\hbar^4 \gamma_1'}{18m_0} (9C_1^2 + 2C_2^2 + 3C_5^2) \\ &\quad - \frac{\hbar^4 \gamma_2}{18m_0} (24C_1C_2 - 4C_2^2 - 3C_5^2) \\ &\quad - \frac{\hbar^4 \gamma_3}{12m_0} C_5 (24C_1 - 4C_2 - 3C_5) \end{aligned} \quad (\text{E8a})$$

$$\begin{aligned} \frac{\Omega_3}{k_0^2} &= \frac{\hbar^3}{3m_e} C_2 \\ &\quad - \frac{\hbar^4 \gamma_1'}{72m_0} (24C_1C_2 - 4C_2^2 - 3C_5^2) \\ &\quad + \frac{\hbar^4 \gamma_2}{3m_0} (3C_1^2 - 2C_1C_2 + C_2^2 - C_5^2) \\ &\quad - \frac{\hbar^4 \gamma_3}{24m_0} C_5 (12C_1 - 2C_2 + 3C_5) \end{aligned} \quad (\text{E8b})$$

$$\begin{aligned} \frac{\Omega_5}{k_0^2} &= \frac{\hbar^3}{m_e} C_5 \\ &\quad - \frac{\hbar^4 \gamma_1'}{24m_0} C_5 (24C_1 - 4C_2 - 3C_5) \\ &\quad - \frac{\hbar^4 \gamma_2}{12m_0} (12C_1C_5 - 2C_2C_5 + 3C_5^2) \\ &\quad + \frac{\hbar^4 \gamma_3}{24m_0} (72C_1^2 - 24C_1C_2 - 36C_1C_5 \\ &\quad - 16C_2^2 - 12C_2C_5 + 27C_5^2) \end{aligned} \quad (\text{E8c})$$

- 
- [1] G. Wannier, Phys. Rev. **52**, 191 (1937).  
[2] R. Elliott, in *Polarons and Excitons*, edited by C. Kuper and G. Whitefield (Oliver and Boyd, Edinburgh, 1963) pp. 269–293.  
[3] R. Knox, *Theory of excitons*, edited by H. Ehrenreich, F. Seitz, and D. Turnbull, Solid State Physics Supplement, Vol. 5 (Academic, New York, 1963).  
[4] R. Knox and D. Dexter, *Excitons* (Wiley, New York, 1981).  
[5] N. O. Lipari and M. Altarelli, Phys. Rev. B **15**, 4883 (1977).  
[6] M. L. Cohen and T. K. Bergstresser, Phys. Rev. **141**, 789 (1966).  
[7] N. O. Lipari, Il Nuovo Cimento B **23**, 51 (1974).  
[8] F. Schöne, S. O. Krüger, P. Grünwald, H. Stolz, S. Scheel, M. Aßmann, J. Heckötter, J. Thewes, D. Fröhlich, and M. Bayer, Phys. Rev. B **93**, 075203 (2016).  
[9] S. Zielińska-Raczyńska, G. Czajkowski, and D. Ziemkiewicz, Phys. Rev. B **93**, 075206 (2016).  
[10] A. Baldereschi and N. O. Lipari, Phys. Rev. B **3**, 439 (1971).  
[11] A. Baldereschi and N. O. Lipari, Phys. Rev. B **9**, 1525 (1974).  
[12] A. Baldereschi and N. O. Lipari, Phys. Rev. B **8**, 2697 (1973).  
[13] M. Altarelli and N. O. Lipari, Phys. Rev. B **15**, 4898 (1977).  
[14] C. Uihlein, D. Fröhlich, and R. Kenkies, Phys. Rev. B **23**, 2731 (1981).  
[15] E. Gross and I. Karryjew, Dokl. Akad. Nauk. SSSR **84**, 471 (1952).  
[16] T. Kazimierzczuk, D. Fröhlich, S. Scheel, H. Stolz, and

- M. Bayer, *Nature* **514**, 343 (2014).
- [17] M. Aßmann, J. Thewes, D. Fröhlich, and M. Bayer, *Nat. Mater.* (2016), doi:10.1038/nmat4622.
- [18] F. Schweiner, J. Main, and G. Wunner, *Phys. Rev. B* **93**, 085203 (2016).
- [19] M. Feldmaier, J. Main, F. Schweiner, H. Cartarius, and G. Wunner, arXiv:1602.00909 (2016).
- [20] J. Thewes, J. Heckötter, T. Kazimierczuk, M. Aßmann, D. Fröhlich, M. Bayer, M. A. Semina, and M. M. Glazov, *Phys. Rev. Lett.* **115**, 027402 (2015), and Supplementary Material.
- [21] H. Mattausch and C. Uihlein, *phys. stat. sol (b)* **96**, 189 (1979).
- [22] F. Schweiner, J. Main, G. Wunner, D. Fröhlich, and M. Bayer, (to be published).
- [23] G. Dasbach, D. Fröhlich, R. Klieber, D. Suter, M. Bayer, and H. Stolz, *Phys. Rev. B* **70**, 045206 (2004).
- [24] G. Dasbach, D. Fröhlich, H. Stolz, R. Klieber, D. Suter, and M. Bayer, *phys. stat. sol (c)* **2**, 886 (2005).
- [25] C. Klingshirn, *Semiconductor Optics*, 3rd ed. (Springer, Berlin, 2007).
- [26] A. Abragam and B. Bleaney, *Electron Paramagnetic Resonance of Transition Ions* (Clarendon Press, Oxford, 1970).
- [27] J. Luttinger, *Phys. Rev.* **102**, 1030 (1956).
- [28] J. Hodby, T. Jenkins, C. Schwab, H. Tamura, and D. Trivich, *J. Phys. C: Solid State Phys.* **9**, 1429 (1976).
- [29] O. Madelung and U. Rössler, eds., *LandoltBörnstein*, New Series, Group III, Vol. 17 a to i, 22 a and b, 41 A to D (Springer, Berlin, 1982-2001).
- [30] M. French, R. Schwartz, H. Stolz, and R. Redmer, *J. Phys.: Condens. Matter* **21**, 015502 (2009).
- [31] U. Rössler, *Solid State Theory*, 2nd ed. (Springer, Berlin, 2009).
- [32] J. Luttinger and W. Kohn, *Phys. Rev.* **97**, 869 (1955).
- [33] K. Cho, *Phys. Rev. B* **14**, 4463 (1976).
- [34] U. Rössler and H.-R. Trebin, *Phys. Rev. B* **23**, 1961 (1981).
- [35] G. M. Kavoulakis, Y.-C. Chang, and G. Baym, *Phys. Rev. B* **55**, 7593 (1997).
- [36] A. Edmonds, *Angular momentum in quantum mechanics* (Princeton University Press, Princeton, 1960).
- [37] J. Broeckx, *Phys. Rev. B* **43**, 9643 (1991).
- [38] S. Rudin and T. L. Reinecke, *Phys. Rev. B* **66**, 085314 (2002).
- [39] M. A. Caprio, P. Maris, and J. P. Vary, *Phys. Rev. C* **86**, 034312 (2012).
- [40] E. Anderson, Z. Bai, C. Bischof, S. Blackford, J. Demmel, J. Dongarra, J. D. Croz, A. Greenbaum, S. Hammarling, A. McKenney, and D. Sorensen, *LAPACK Users' Guide*, 3rd ed. (Society for Industrial and Applied Mathematics, Philadelphia, PA, 1999).
- [41] J. Cederberg, *Am. J. Phys.* **40**, 159 (1972).
- [42] G. Dasbach, D. Fröhlich, H. Stolz, R. Klieber, D. Suter, and M. Bayer, *Phys. Rev. Lett.* **91**, 107401 (2003).
- [43] M. Kanehisa, *Physica B+C* **117-118**, 275 (1983).
- [44] J. Zamastil, F. Vinette, and M. Šimánek, *Phys. Rev. A* **75**, 022506 (2007).